SPIROGRAPH TOY MODELLING USING TWO-LINK PLANAR ROBOTIC ARM IN MATLAB

Rajkishore Prasad

Principal, B. N. College, Patna
Ashok Rajpath, Bihar State 800004, India
profrkishore@yahoo.com

Shivanshu Raj

Student, Deptt of Computer Science and Engineering
SRM University, Andhra Pradesh
rajshivanshu19@gmail.com

Abstract

This paper presents modelling of a physical Spirograph Toy, a mathematical instrument for the curve generation of roulette family, using two-link planar robotic arm whose forward kinematic equations can yield parametric equations of the trochoid or spirographic family of curves if both joints are rotated simultaneously respecting a proportional relation. The software version of spirograph toy was simulated in MATLAB using two-link planar robotic manipulator having all joints revolute type and spirograph curves were obtained for different parameters values. Here cases of different patterns of spirograph curves such as hypocycloid, hypotrochoid, epicycloid and epitrochoid are dealt with examples. The generated curves were found in agreement with that of generated by parametric equations and a physical spirograph toy. The implemented soft version of spirograph provides scope for selecting multiple trace points at different positions, even beyond the region of rolling disc, simultaneously which is not possible with the physical spirograph toy. In the digital version of spirograph, it has been found possible to draw a fixed-frame crossing spirograph which is not possible to complete with the physical spirograph toy and this practicability makes digital version of spirograph superlative while providing feeling of physical spirograph motion in the course of obtaining spirograph drawings. The proposed robotic model was also used to draw spirograph of fixed size but of the same shape as that of produced by spirographic motion using inverse kinematics and Affine transform. Such a model can be used further to make spirographs on wood frame or walls for decoration.

Keywords: Spirograph, Two-arm robot, Hypotrochoid, Epitrochoid, Curve generation.

1. Introduction

Spirograph has been one of the most common toys of childhood of most of us across the globe. Although this toy is very cost-effective and simple in construction and use, but generates beautiful and attractive patterns of curves creating impression of magic. As shown in the Fig. 1(a), the spirograph set consists of a fixed bigger circular frame and many smaller circular teethed discs of different radii with patterns of holes through which pen or pencils can be inserted to rotate the disc along the teethed internal or external edges of the fixed circular frame such that the inserted pen/pencil also traces locus of pen-point ensuring slip free roll of disc. The curve so generated are called spirographs or spirographic curve. Although it looks very simple in design, but its tale of invention is not a one man-show and starts with the effort of Swiss mathematician Johann Samuel Eberhardt who thought for design of a machine for drawing and after that there come names of many scholars who contributed in the invention of spirograph [1], however, the spirograph as the mathematical instrument was invented by Polish mathematician Bruno Abdank-Abakanowicz between 1881 and 1900 for drawing spirals and that was also modified later by many others. Finally, a gear based spirograph came into existence since 1908 after advertisement of Marvelous Wondergraph in Searls catalogue [2,3]. But as a toy it was exhibited by an Engineer Denys Fisher in 1965 which earned many awards including educational toy of the year of U.K [1,4].

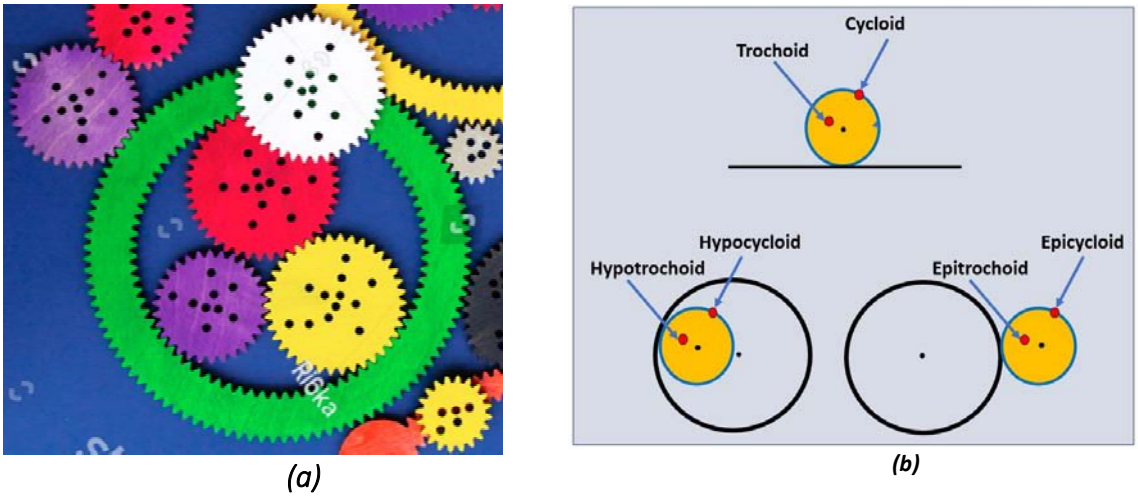

Fig. 1. (a) Spirograph toy with teethed frame and discs having trace point holes (Curtsey: Alamy Stock Photo) (b) Nature and names of curves generated by spirograph toy.

In 1600, Galileo first coined the term cycloid to describe the locus of the point lying on the perimeter of the circle rolling over a straight line and when the trace-point lies inside or beyond the perimeter of rolling circle the locus of the curve was named trochoid. In the spirograph, the smaller circle is rolled along the outer or inner edge of a circle and accordingly curves generated as the locus of the tracing points and are called hypocycloid when trace-point is on the perimeter and a hypotrochoid if the tracing point is within or beyond the territory of rolling circle. If the point is within the radius of the inner circle, the curve is called a curtate hypotrochoid. In case if trace point is beyond the periphery of rolling circle, it is called a prolate hypotrochoid. If the rolling circle rolls along the outer edge of the fixed circle, the curves are called respectively epicycloid and epitrochoid for related locations of traces point as shown in the Fig. 1(b). If the point is within the radius of the inner circle, the curve is called a curtate epitrochoid. In case if the trace point is off the rolling circular disc, it is called a prolate epitrochoid.

The spirograph seems to be a toy but in fact it is a mathematical instrument that generates curve known as spirographs and are subset of the Roulette family of curve [5,6]. These curves are very important in engineering and scientific research as such curves have been found as the locus trace of many physical events. In the very brief account of such examples, the first is from the ancient Greek model, in both Hipparchian and Ptolemaic systems [7,8], of solar system which was based on epicyclic motion. In another interesting research investigation in [9], authors have observed and reported hypocycloidal and epicycloidal motion of irregular grains of pine pollen in unmagnetized dust plasma in 2D plane. In [10], based on very old eponymous Bertrand's theorem the shape of the orbit trajectory for a body moving under the power law has been found to be spirograph like (both of crossing and non-crossing hypocycloidal and epicycloidal patterns). In [11,12], an important application of cycloid curve has been presented where in a cycloid gear box, being used as speed reducer/amplifier in the mechanical power transmission, has been discussed. Similarly, in [13] optimal bus door opening mechanism has been studied using hypocycloids. The detailed discussion on use of spirograph like curves and pattern in Arts has been presented in [14]. Even in modern time some architectural designs in buildings are often seen that use such curve and surface innovation [15]. In [16], authors have proposed a mixing device based on hypotrochoid motion to produce pseudo-Anosov mixings solutions of viscus fluid. In the field of autonomous robot navigation authors in [17] have used hypocycloid to ensure collision free and decoupled path planning for multi-robot and have found it superior in performance. The other real example of spirograph like motion trajectory is found in the magnetrons and in electron beam focusing devices wherein perpendicular electric and magnetic fields are used to control charged particle motion under which moving charged particle beam follow epitrochoidal or hypocycloidal paths [18] depending upon the initial velocity, magnitude, and directions of charged particles. In [19], researchers have reported that the trajectory of a charged test particle in the Melvin magnetic universe takes the shape of hypocycloids which is parametrised by the magnetic flux strength of the Melvin space-time. In another interesting application [20] a hypocycloidal motor using two-harmonic field in the airgap have been proposed and investigated to show improved performance with added simplicity. In a research report in [21], researchers have characterised roots of univariant trinomials in the patterns of trochoidal curves. In an interesting research, as reported in [22], authors have used spirograph patterns to represent ecological weighted network termed as Eco-Spiro-Vis to represent flow of energy and matter within species in eco-system. In another very interesting research report in [23], authors have proposed to use modified, using visual composition techniques, spirograph patterns for tweet display or other relatively large time-oriented datasets. In the research area of path design for multiple robotic agents in [24], the researchers have proposed use of complex trochoidal path for the coordinated,

distributed and obstacle free movements. The development of spirograph based mechanical system has been reported in [25]. These are some of the important applications of spirographic patterns presented to make account of its importance in engineering and science.

Although the spirograph appeared as a toy in the marketplace in 20th century in physical form, at present it is very popular in digital forms [26,27,28,29,30,31]. The different versions of drawing robots are being marketed to draw curves and their attractive patterns. However, these models lack spirograph like geometric design style and fail to demonstrate natural roll and trace motion of a spirograph. Using the parametric equations of spirograph curves one can obtain spirograph curve patterns but cannot get in-depth understanding and visualization of its generation process which a physical spirograph provides. But, physical spirograph has many limitations, for example, it cannot be used to draw spirograph for off the disc trace-points, it cannot complete graph if selected pen-point needs to cross fixed frame boundary, it requires change in size of spirograph frame size for change in the size of spirograph, it is in convenient to keep different size of smaller disc etc. In fact, one cannot draw precise hypocycloid or epicycloid for given parameters as the required trace point hole cannot be made on the edge of rolling disc. Thus, there is need of developing a robotic model that can mitigate such problems and can be used to draw spirograph patterns for decoration on walls, wood plate glass plate etc. to meet the commercial needs.

In the present study, our aims are on the similar ways i.e. to develop its soft version which can involve user like a physical spirograph and propose to use robotic technology to design a two-arm robot that can draw spirographic curve describing roll motion like that of a physical spirograph set. Accordingly, this paper is divided in many sections to present our efforts. In the next section robotic modelling and simulation of spirograph in MATLAB are presented. In the section III, some important parameters and shape of the spirograph are dealt with discussion on different spirographs patterns drawn by robotic arm. The section IV presents conclusions and discussion on the future work. Then this paper ends with some references.

2. Robotic Modelling of Spirograph

The study on mathematical modelling of spirograph toy has been done by many scholars in the past and parametric equations for the trajectory of trace point have been obtained which can be used to generate spirographic curves [28,32,33,34]. In [29], it was modelled using the general Farris Equation too. But here we model spirograph toy as a two-arm planar robot and using forward kinematic equation of the two-linked robotic arm, the spirograph patterns are obtained. In a spirograph toy, as shown in the Fig. 2, when a smaller circular disc of radius r rolls along the outer or inner edge of fixed circular frame of radius R, the center of the rolling circular disc moves on a circle of radius $L_1 = (R - r)$ or $L_1 = (R + r)$ respectively for roll along inner or outer edge. As the discs behaves like a rigid body, the motion of the smaller disc can also be described in terms of two-link planar manipulator with first link length L_1 and second link length $L_2 = h$, joined together at O_2 with revolute joint, wherein $L_2 = h$ represents distance of tracing point from the centre of rolling disc. In this model the length of second link will depend upon the location of selected trace point and thus varies. When the smaller disc rotates it decides shift in its center on the circular path in a direction opposite to its own rotation for inner rolls. Accordingly, the imagined first link also rotates. The existence of first link and joints are also not vivid. In a real spirograph toy neither L_1 nor such link pair is visible and available but rotation and roll happens due to traction at pen-point as if such mechanism exists and thus assumption and insertion of such two links makes sense and simplifies the picture of motion mechanism of spirograph toy.

Thus, spirograph motion can be understood as that of two-link planar manipulator in which links are invisible directly but the relative motion of rotation due to rolling of smaller disc along the inner or outer edge of fixed frame circle results in proportional rotation of imagined first link L_1 too.With such a robot-like model with two revolute joints at O_1 and O_2, the coordinates of trace point can be obtained as the function of joint angles using forward kinematics. As shown in the Fig.2, let us attach a global frame of reference at the joint O_1 and at any time instant the link L_1 is at angular displacement θ_1 and the link L_2 makes angle θ_2 from link L_1 or the positive x-axis of reference frame $\Sigma O_0 X_1 Y_1$. The coordinates (x_2, y_2) of pen-point P in frame $\Sigma O_2 X_2 Y_2$ is given by

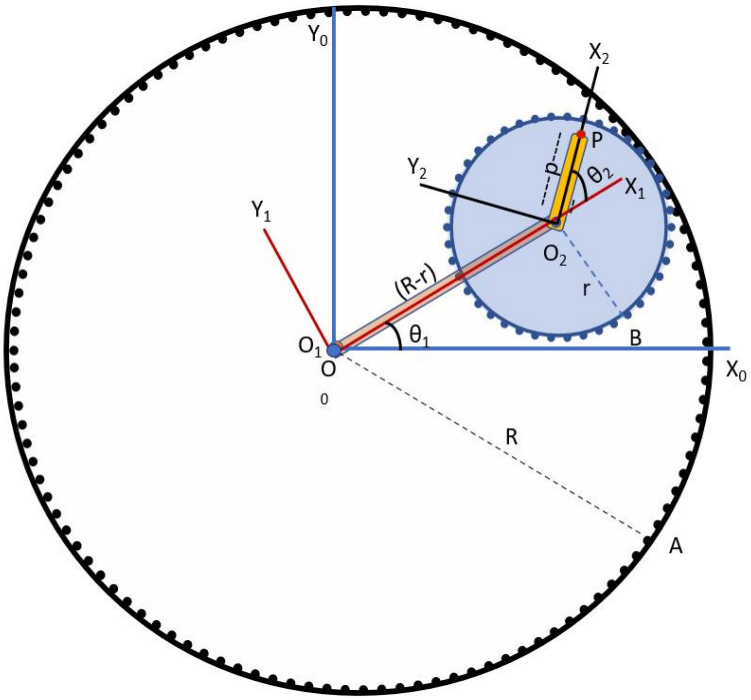

Fig. 2. Modelling of Spirograph as two-link planar manipulator.

$$P_2 = \begin{bmatrix} x_2 \\ y_2 \end{bmatrix} = \begin{bmatrix} h \\ 0 \end{bmatrix}. \tag{1}$$

The coordinate (x_0, y_0) of trace point P can be expressed in base reference $\Sigma O_0 X_0 Y_0$ using following transformation equation

$$\begin{aligned} P_0 = \begin{bmatrix} x_0 & y_0 \end{bmatrix}^T &= R_{01}\left[R_{12}P_2 + T_{12}\right] + T_{01} \\ &= [R_{01}R_{12}P_2 + R_{01}T_{12}] + T_{01} \end{aligned} \tag{2}$$

where R_{01} = rotation matrix for frame ΣO_1 to ΣO_0,
R_{12} = rotation matrix for frame ΣO_2 to ΣO_1,
T_{01} = translation matrix for frame ΣO_1 to ΣO_0,
T_{12} = translation matrix for frame ΣO_2 to ΣO_1.

These rotation and translation matrices, considering plane motion in x-y plane *i.e. z=0*, for Fig. 2 are given as

$$R_{01} = \begin{bmatrix} \cos\theta_1 & -\sin\theta_1 \\ \sin\theta_1 & \cos\theta_1 \end{bmatrix}, \quad R_{12} = \begin{bmatrix} \cos\theta_2 & -\sin\theta_2 \\ \sin\theta_2 & \cos\theta_2 \end{bmatrix}, T_{01} = \begin{bmatrix} 0 \\ 0 \end{bmatrix} \ \& \ \ T_{12} = \begin{bmatrix} R-r \\ 0 \end{bmatrix} \tag{3}$$

Now the spirograph curves are set of coordinates of tip of the rotating link L_2 in the base coordinate frame which can be obtained by using Eq.1 and Eq. 3 in Eq. 2 as follows

$$P_0 = \begin{bmatrix} x_0 \\ y_0 \end{bmatrix} = \begin{bmatrix} C\theta_1 & -S\theta_1 \\ S\theta_1 & C\theta_1 \end{bmatrix} \begin{bmatrix} C\theta_2 & -S\theta_2 \\ S\theta_2 & C\theta_2 \end{bmatrix} \begin{bmatrix} h \\ 0 \end{bmatrix} + \begin{bmatrix} C\theta_1 & -S\theta_1 \\ S\theta_1 & C\theta_1 \end{bmatrix} \begin{bmatrix} R-r \\ 0 \end{bmatrix} + \begin{bmatrix} 0 \\ 0 \end{bmatrix}$$

$$= \begin{bmatrix} hC(\theta_1+\theta_2) \\ hS(\theta_1+\theta_2) \end{bmatrix} + \begin{bmatrix} C\theta_1(R-r) \\ S\theta_1(R-r) \end{bmatrix} = \begin{bmatrix} (R-r)C\theta_1 + hC(\theta_1+\theta_2) \\ (R-r)S\theta_1 + hS(\theta_1+\theta_2) \end{bmatrix}.$$

Obviously,

$$\begin{aligned} x_0 &= (R-r)Cos\theta_1 + hCos(\theta_1+\theta_2) = L_1Cos\theta_1 + L_2Cos(\theta_1+\theta_2). \\ y_0 &= (R-r)Sin\theta_1 + hSin(\theta_1+\theta_2) = L_1Sin\theta_1 + L_2Sin(\theta_1+\theta_2). \end{aligned} \tag{4}$$

Palpably, spirograph can be obtained as the locus of trace point P which is also tip or end-effector of the two-link planar robot whose coordinates (x_0, y_0) in the base frame are given by Eq. (4) as the function of joint angles. Thus, the spirographic motion can be described using forward kinematics of a two-arm planar robot having both joints of revolute type with first arm length L_1, the distance of center of rolling circle from the center of fixed circle, and second arm length $L_2 = h$, the distance of pen-point from the center of rolling circle. The tip of the first link L_1 ends at the center of rolling circle and that of 2nd link L_2 ends at pen point. However, such a link pair of L_1 and L_2 is not visible explicitly in the real spirograph instruments but can be imagined and motion of a spirograph can be described in terms of so imagined two-link planar robot as mentioned above. The center of the rolling circle makes revolution on a circumference of a circle of radius L_1 and the angular displacement of θ_1 in link L_1 is produced by and related to angular displacement θ_2 of the rolling circle. Their relation can be expressed in terms of the ratio R/r which represents number of rotations required to be completed by smaller circle to complete one roll along the edge of frame circle. This in turn implies that $2\pi R/r$ rad rotations of smaller circle bring 2π rad of rotations in link L_1. Thus, the rotation of θ_2 rad in smaller circle is related to corresponding rotation of θ_1 rad in L_1 such that

$$R\theta_1 = r\theta_2 \Rightarrow \theta_1 = \frac{r}{R}\theta_2. \tag{5}$$

Geometrically, the clockwise rotation of a smaller circle about its center O_2 leads to anti-clock wise roll along inner edge and vice-versa. However, for the roll along outer edge of the fixed frame, the directions of rotations in L_1 and L_2 are same. The situation of roll along inner edge is shown in Fig. 3(a) in which trace-point P lies initially on *X*-axis and the smaller circle is given clockwise rotation by β rad about O_2 which results in rotation of α rad about O_1. The geometry of Fig.3(a) gives here $\theta_2 = 2\pi - \beta$ and $\theta_1 = \alpha$ use of which in Eq. (4) gives

$$\begin{aligned} x_0 &= (R-r)Cos\alpha + hCos(2\pi+\alpha-\beta) \\ &= (R-r)Cos\alpha + hCos(\alpha-\beta) = (R-r)Cos\frac{r}{R}\beta + hCos\left(\frac{r-R}{R}\right)\beta \\ &= (R-r)Cos\frac{r}{R}\beta + hCos\left(\frac{R-r}{R}\right)\beta = (R-r)Cos\alpha + hCos\left(\frac{R-r}{r}\right)\alpha \end{aligned} \tag{6}$$

$$\begin{aligned} y_0 &= (R-r)Sin\alpha + hSin(2\pi+\alpha-\beta) \\ &= (R-r)Sin\alpha + hSin(\alpha-\beta) = (R-r)Sin\frac{r}{R}\beta + hSin\left(\frac{r-R}{R}\right)\beta \\ &= (R-r)Sin\frac{r}{R}\beta - hSin\left(\frac{R-r}{R}\right)\beta = (R-r)Sin\alpha - hSin\left(\frac{R-r}{r}\right)\alpha \end{aligned} \tag{7}$$

These equations represent coordinates of spirographic family of curves known as hypotrochoid.

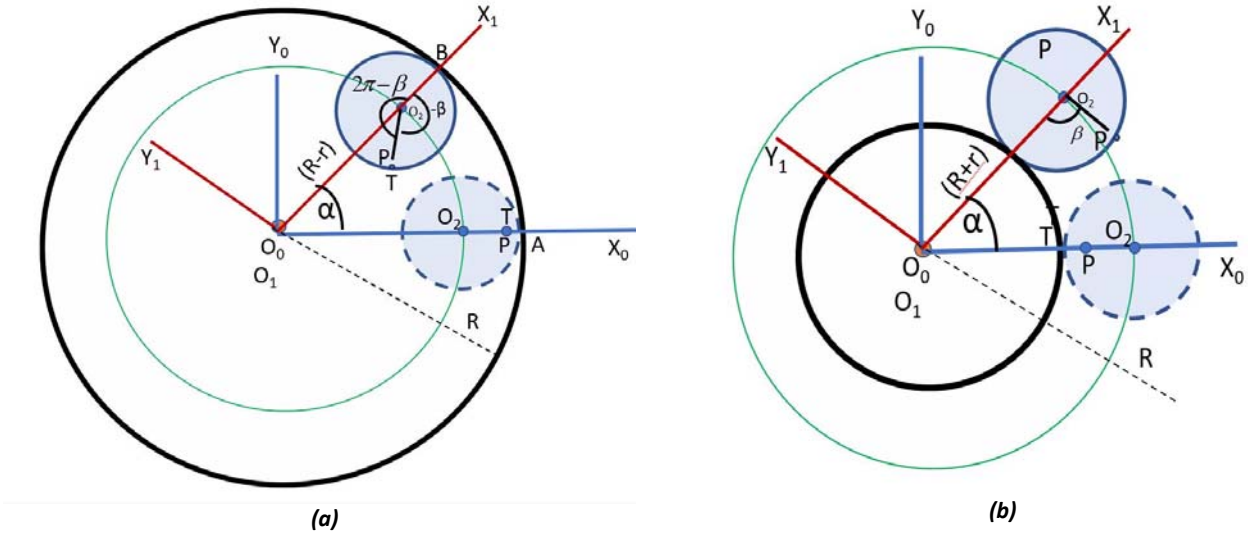

Fig. 3. (a) The hypocycloid/hypotrochoid curve generation due to roll of smaller circle along the inner edge of frame circle (b) The epicycloid/epitrochoid curve generation due to roll of smaller circle along the outer edge of frame circle.

The geometric situation of roll of smaller circle along the outer edge of the fixed circle is drawn in Fig. 3(b) in which the trace point *P* is initially on the x-axis as is shown. When the trace point suffers rotation of $\beta\ rad$ about O_2 in the anticlockwise direction, the smaller circle also rolls along outer edge of fixed circle in anticlockwise direction. As shown in the same figure, its center makes revolutions on a circle of radius $L_1 = (R + r)$ and the equation of resulting curve as the locus of trace-point is known as epitrochoid if trace point is not on the circumference of the rolling disc and epicycloid if the trace point lies on the circumference of the rolling disc. From the geometry of Fig. 3(b), we have $\theta_2 = \pi + \beta$ and $\theta_1 = \alpha$ and use of these values in Eq. (4) gives

$$x_0 = (R+r)Cos\alpha + hCos(\pi + \alpha + \beta) = (R+r)Cos\alpha - hCos(\alpha + \beta)$$
$$= (R+r)Cos\frac{r}{R}\beta - hCos\left(\frac{r+R}{R}\right)\beta = (R+r)Cos\alpha - hCos\left(\frac{r+R}{r}\right)\alpha \quad (8)$$
$$y_0 = (R+r)Sin\alpha + hSin(\pi + \alpha + \beta) = (R+r)Sin\alpha - hSin(\alpha + \beta)$$
$$= (R+r)Sin\frac{r}{R}\beta - hSin\left(\frac{r+R}{R}\right)\beta = (R+r)Sin\alpha - hSin\left(\frac{r+R}{r}\right)\alpha \quad (9)$$

These are coordinates for parametric equation of epitrochoid which is same as the coordinates of tip of two-link robotic manipulator. Thus, the two-link manipulator can be used to plot spirographic family of curves such as hypocycloid, hypotrochoid, epicycloid and epitrochoid.

2.2 Simulation of Robotic Model of Spirograph

The two-arm planar manipulator model of spirograph was implemented in MATLAB. The screenshot of developed GUI is shown in Fig. 4. This GUI contains sliders and boxes to set different parameters such as $R, r,$ angular velocity of rotation of smaller circle, resolution of graph, number of revolutions etc. as shown in the GUI panel. User can select location of pen/trace points using mouse click by clicking pen point. In the physical toy of spirograph the two limitations namely selection of pen points off the smaller disc territory and selection of multiple tracing points for simultaneous drawing are very frustrating and cannot be done. However, in the soft versions, presented here, both are possible and spirograph can be drawn. In the current setting ten tracing points can be selected at the same time and that limit can be increased. The GUI also contains a push button for drawing parametric equation directly for inner or outer roll. The pop-down menu under select to plot can be used to plot spirograph and joint angles of both revolute joints of the two-link planar robot.

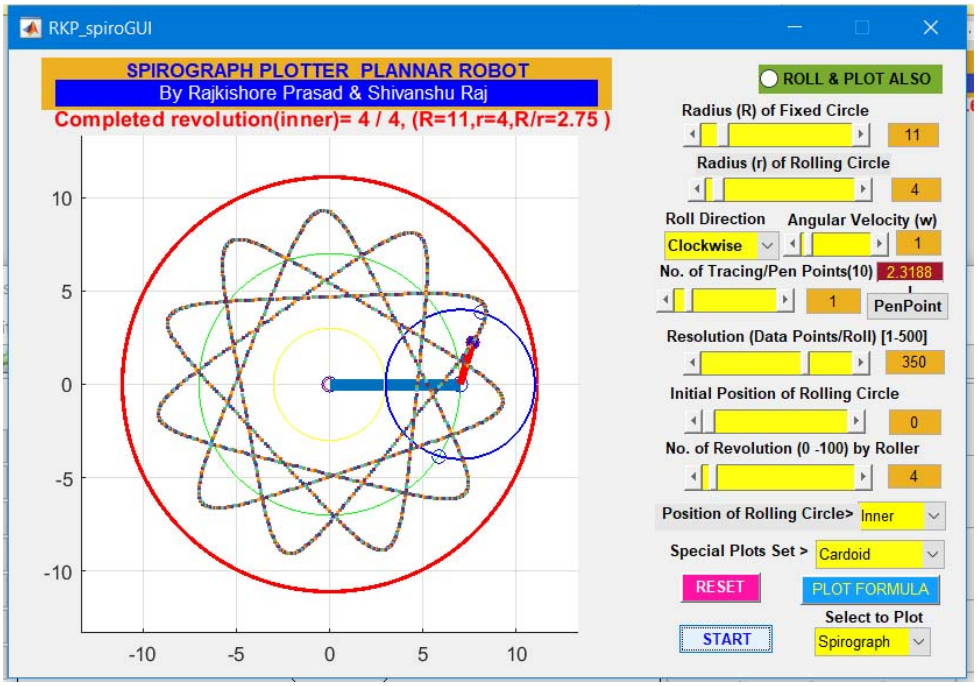

Fig. 4. Showing screenshot of GUI developed for the spirographic plannar robot.

3. Results and Discussion

As it is obvious that the spirograph equations are functions of structural parameters (R, r, h, β) and edge (outer/inner) along which smaller disc rolls but the visual look of the generated curves depends on ratio R/r, edge of roll and distance of pen-point from the centre of rolling disc. For $h = 0$, the coordinates (x_0, y_0) represent circle as is also obvious from Eq.(4) and for increased value of h the shape of the spirograph changes and cusps, which are outward projections in hypotrochoid and inward projections in epitrochoids, begin to appear in a number depending on the ratio R/r. A cusp is formed for each revolution of

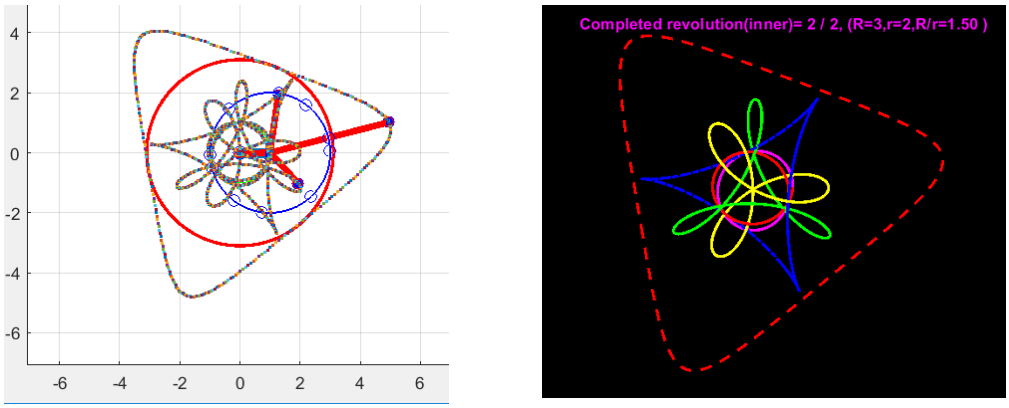

Fig. 5. Spirograph for $h = 0$ & $h \neq 0, R = 3$ and $r = 3$ units As the value of h increases the sharpness of corners decreases and curve tends to become circular.

rolling disc as is shown in Fig. 5. The number of revolutions by the smaller disc required to coincide with the starting position of the tracing point is known as the period of spirograph pattern and it is determined by the ratio R/r and distance of tracing point from the centre of rolling circle. The smallest reduced fraction of R/r gives the

number of cusps, period and design and behaviour pattern near cusps [1]. In the reduced fraction ratio $m/n = R/r$, numerator m gives number of cusps and n represents period of the spirograph curve. If R/r represents an irrational number then the spirograph will have no period meaning thereby spirograph remains open. So, if $(R/r) = k$ the parametric equations for Epitrochoid and Hypocycloid can be expressed as

For epitrochoid

$$x_0 = r(k+1)cos\alpha - hcos(k+1)\alpha;\ \ y_0 = r(k+1)sin\alpha - hsin(k+1)\alpha, \tag{10}$$

and for hypotrochoid

$$x_0 = r(k-1)cos\alpha + hcos(k-1)\alpha;\ \ y_0 = r(k-1)sin\alpha - hsin(k-1)\alpha. \tag{11}$$

These parametric equations can also be used to generate spirograph curves as has been done in [29] but that does not exhibit the way in which spirographic curves are generated. Usual spirographs are complex geometric design due to multiple symmetry. Both the rotational and reflection types of symmetry groups are present in the spirograph, so cyclic and dihedral group symmetries are obvious with modality that same design structures with different representation can be found in the same group [33]. Thus, only formulae or parametric equation plotting, done to present results, provides picture of shape of the curve but for more satisfactory and in-depth understanding of curve generation process and its visualization is essential and that can be done using the proposed robotic model in a very convenient way. The complexity increases when multiple spirographs are drawn in the same figure. Accordingly, selection of multiple trace points can also be visualized conveniently using proposed robotic model.

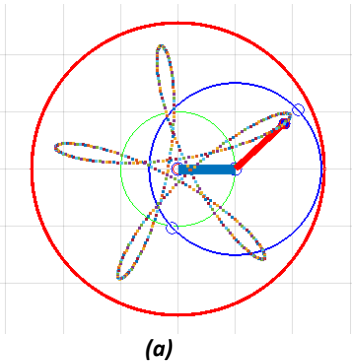
(a)

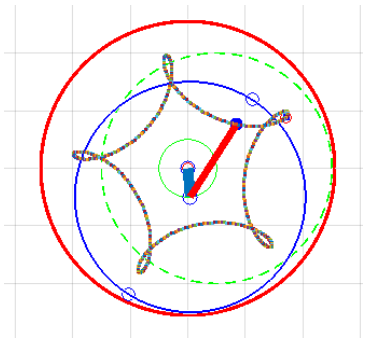
(b)

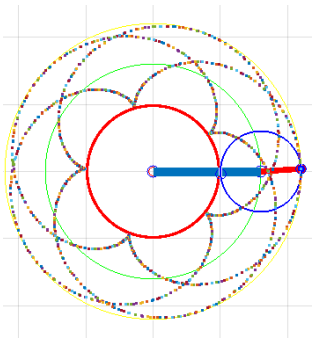
(c)

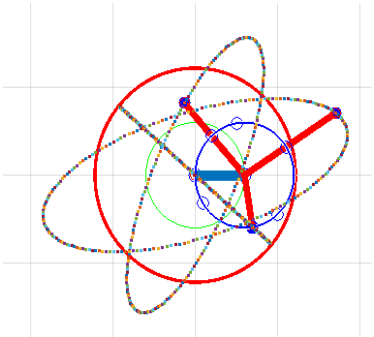
(d)

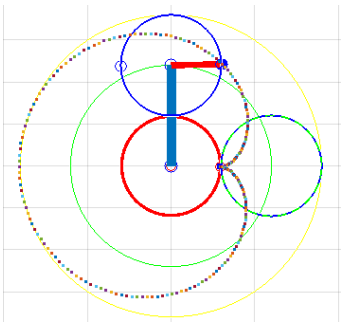
(e)

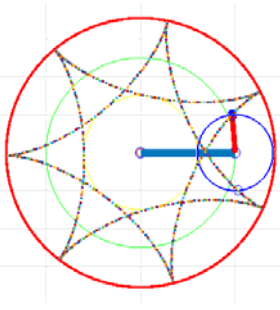
(f)

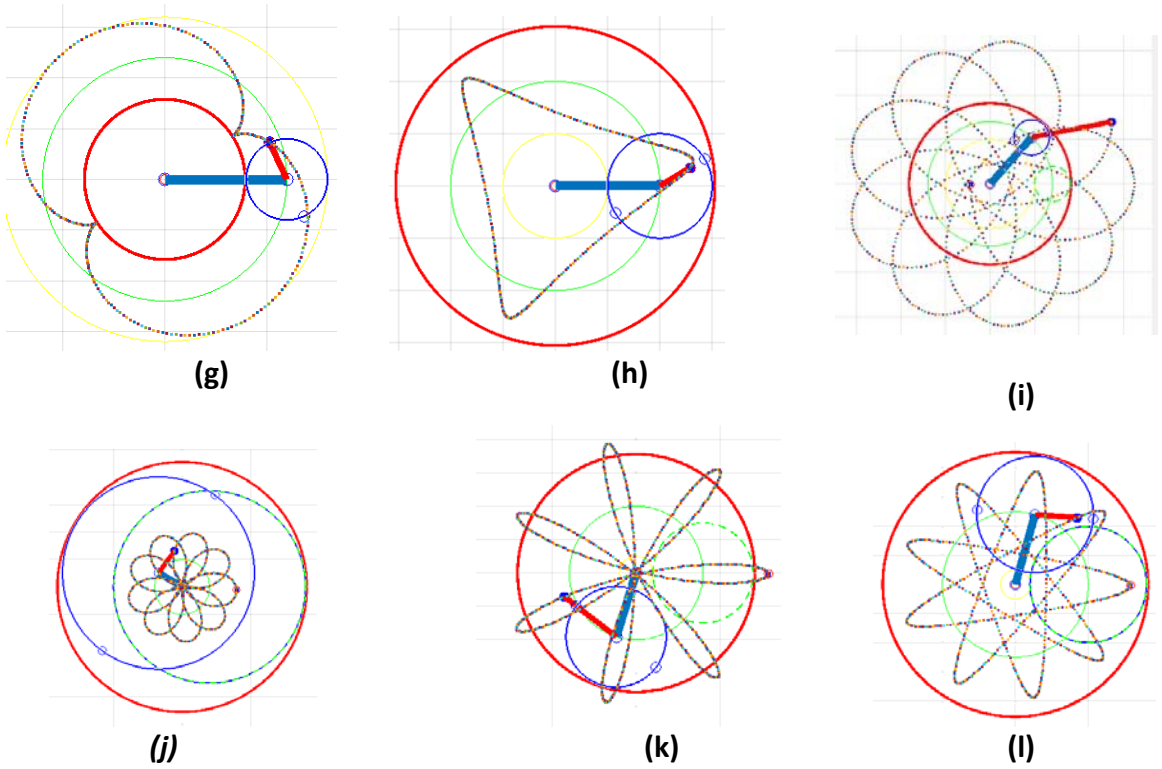

Fig. 6. Spirographs (a) $R/r = 5/3$ *hypotrochoid* (b) $R/r = 5/4$ *hypotrochoid* (c) $R/r = 5/2$ *epicycloid* having dihedral Group symmetry (d) multiple trace points for $R/r = 2, h = r$ a straight-line segment called Tusi Couple and for $R/r = 2, h \neq r$ Ellipse (e) Cardioid for *R=r=h* (f) Asteroid for *R=7, r=h=2* (g) Nephroid *R/r=2* (h) Deltoid for R/r=3. (i) Rosetta orbit shaped hypotrochoid for $R = 9, r = 2, h = 9.19$ unit (j) Rose curve or *Rhodonea family* of curves drawn by two arm robot as Hypotrochoid with structural parameter $(R = 9, r = 7 \,\&\, h = 2\ units)$ (k) Rose Curve Drawn by two arm robot as Hypocycloid with structural parameter $(R = 7, r = 3 \,\&\, h = 4\ units)$ (l) Star or Polygram hypotrochoid obtained with structural parameter $(R = 9, r = 4 \,\&\, h = 2.8\ units)$.

As said before that the spirograph curves are mathematically hypotrochoids and epitrochoids which have some well-known and earmarked shapes for some structural parameters of the spirograph instrument. For example, Tusi Couples, Ellipse, Asteroids, Deltoids, Cardioids, Nephroids etc. which are shown in the Fig. 6 and were drawn using depicted structure parameters of the spirograph. The other very important modification of hypotrochoid curve is into the rose curve or *Rhodonea* family [35] of curves because of its flower petal like shape which are also depicted in the Fig. 6. Obviously, these standard spirographs were obtained using developed robotic model and have been found to be same as that of parametric equation plots.

The changes in the structural parameters of spirograph not only produce changes in shape and overall appearance of the spirograph curves but also bring changes in the curvature of the different parts or points of curves. Thus, the cusp connectivity and nature of curvature suffer change from concave to convex and vice-versa. The avid readers can find details of it in [36]. Two such examples of spirographs are depicted in Fig.7 for the different values of distance of trace-point *P* for both the inner and outer rolls of the rolling disc. It is very interesting to note here that the change in curvature occurs both for hypotrochoid and epitrochoid family of curves. How the curvatures of the curves change gradually at each point can be observed in these figures. The corners can be rounded or pointed. The detailed mathematical analysis of the same is not done here, however, such analysis may be helpful in generating such curves with mobile agents or mobile robots or by some other means as has been presented in [34]. The spirograph plots can be generated in different ways but its application for decorations on walls and other domestic and official items calls for convenient ways and for the same traditional spirograph toy is not suitable as it can draw on plain surface only. With the advancement in the digital computation, the technology of pattern generation has taken huge benefits in the form of the development of different algorithms for the generation of intersecting geometric patterns and trajectories. Similarly, generation of spirograph curves by some mobile agents based on curvature study is very good idea and may be helpful in rendering spirograph on curved surface.

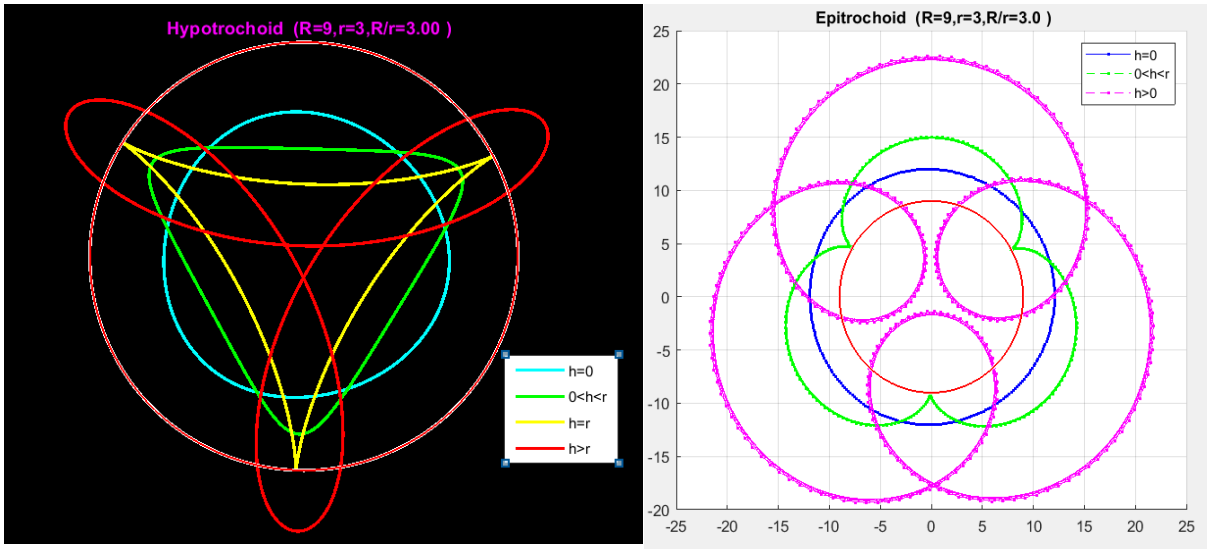

Fig. 7. Change in curvature of spirograph with changes in the structural parameters. (a) change of curvature in hypotrochoid (b) change in curvature in epitrochoid.

As mentioned earlier that using physical spirograph toy, the hypocycloid or epitrochoid whose locus needs to cross fixed-frame circle as well as spirograph-drawing selecting two or more trace points simultaneously cannot be completed, however, authors in [32] suggested some modifications in physical spirograph and obtained even then incomplete epitrochoid curve for $h > r$ with many difficulties and compromises. In the proposed software version of spirograph both of such cases are possible to tackle. In the Fig. 8 such hypotrochoid and epitrochoid have been presented which were drawn selecting multiple tracing points simultaneously. This is one of the biggest benefits of the proposed model that can exhibit completion of fixed-circular frame crossing curves without any break in the visualization of rolling motion of the circle. In the Fig. 8(c) three tracing points were selected for structure parameters $r = R/2, h = r$ and all the three trace-points lie on the circumference of the circular disc. The traced hypocycloid curves are straight line for each trace point. This is very interesting and demonstrates functioning of hypocycloidal straight-line mechanism as elaborated in [37]. Also, some of the curve patterns obtained by spirograph toy have very attractive looks and can be used for decorative purpose. However, it cannot be drawn by hand. Both hypotrochoid and epitrochoid curve have beautiful decorative looks due to repetition of

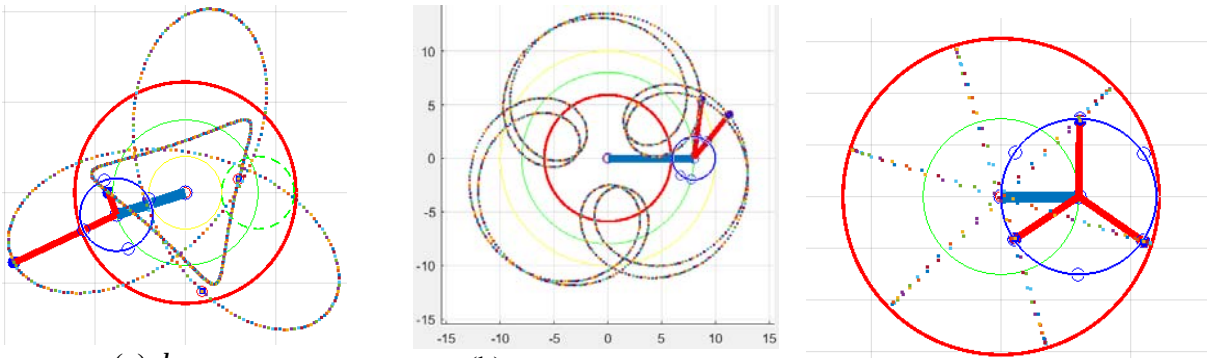

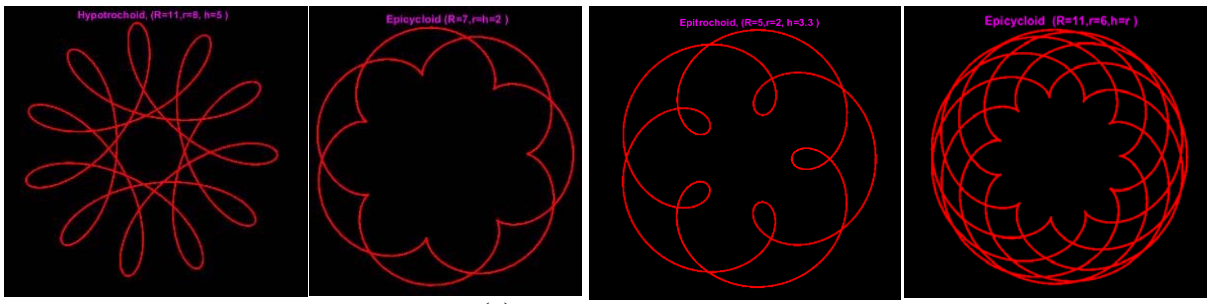

(d) (e) (f) (g)

Fig. 8. (a) Hypotrochoid with trace points $h > r$ and $h < r$ **(b)** Epitrochoid with two tracing points for $h > r$ and $R/r = 3$ **(c)** Hypocycloid to show how the vertices of a triangle move on straight line if they all are co-circular.(c) beautiful spirographs drawn using robotic model **(d)** Hypotrochoid with structural parameters $(R = 11, r = 8 \,\&\, h = 5 \; units)$ **(e)** Epitrochoid with structural parameters $(R = 5, r = 2 \,\&\, h = 3.3 \; units)$ **(f)** Epicycloid with structural parameters $(R = 6, r = h = 1 \; units)$ **(g)** Epicycloid with structural parameters $(R = 11, r = h = 6 \; units)$.

patterns and fractal nature of the curve. Some such attractive patterns are shown in the Fig.8(d-g) which were obtained using different structural parameters.

In the aforesaid robotic model, the plotted spirograph is centered at the center of the fixed circular frame of the spirograph. The spirograph coordinates generated so can be mapped into other coordinate values such that it can be drawn on the other fixed canvas by a robotic arm preserving shape in different sizes. In such a case link length of two-armed robot is kept fixed and spirograph coordinates are transformed so that the shape of the spirograph pattern remains unchanged. However, under such plan of drawing spirograph, the robotic arm does not demonstrate natural rolling pattern of spirograph toy and it moves as per estimated joint angles [38]. According to the supplied coordinate points (x, y) of a spirograph the robot configuration, set of joint angles, for a planar two-arm manipulator with links of lengths l_1 and l_2 is estimated using inverse kinematics and are given by

$$\theta_1 = \tan^{-1}\left(\frac{x}{y}\right) \pm \cos^{-1}\left(\frac{x^2 + y^2 - l_1^2 - l_2^2}{2 l_1 l_2}\right) \; and \; \theta_2 = 180 \pm \cos^{-1}\left(\frac{x^2 + y^2 - l_1^2 - l_2^2}{2 l_1 \sqrt{x^2 + y^2}}\right). \tag{12}$$

These equations yield two sets of joint angles that give reflecting configurations of robotic arm about the line joining end effector and origin. Thus, any set of estimated values of joint angles can be used. The coordinates of spirographs are transformed using Affine Transform [39] with proper scaling and shifting values so that spirograph is fitted in the new canvas dimensions lying within the territory of workspace of robotic arm. An example of such a plot is shown in the Fig. 9 wherein the arm-lengths of simulated robotic manipulator have been kept equal.

4. Conclusions

In this paper the robotic modelling of a spirograph toy using the two-link planar robotic arm with two revolute joints was presented and was shown how the forward kinematic equation could produce spirograph if both joints were rotated following a proportional relation. The model was simulated in MATLAB and a GUI was created to draw spirograph. The developed GUI has been made user friendly and can be used to carry out experiments on spirograph curve either in teaching or in research as it provides option to control and set structure parameters of spirograph. The soft version of the spirograph also provides ways to select trace point at different locations of choice in multiple numbers that are cumbersome in a physical spirograph for the simultaneous drawing. Using inverse kinematic equation, the generated curve points were used to estimate robot configuration to draw spirograph on different canvas. The spirograph curve patterns are very attractive and decorative too. Thus, a real robots can be used to draw such patterns on walls for decorative applications. Such physical robots that can draw spirographs on wall, that can cut spirographic grooves in wooden frame can also be developed for the commercial gain.

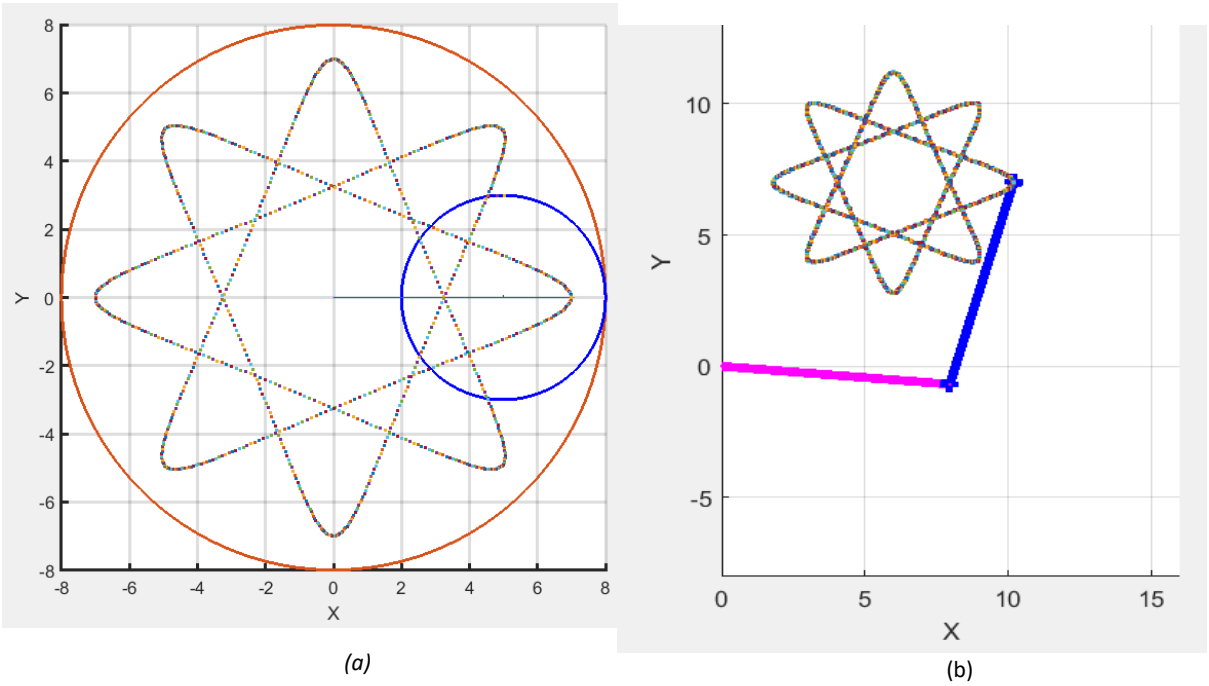

Fig. 9. Mapping of spirograph using Affine Transform to plot in the fixed canvas by a two-arm planar robot with links $l_1 = l_2 = 8$ *units*.

Conflict of Interest

The authors have no conflict of interest to declare. The authors have seen and agreed with the contents of the manuscript.

References:

1. Rachel Evans, The History of Spirograph. Available at: https://www.spirographgirl.com/blog/the-history-of-spirograph
2. P. Nicla, P.Nicolina. Creating new Mathematically-sustainable world(2014): From the spirograph, a reverse path. 13th Conference on Applied Mathematics APLIMAT,. Available at: https://ortus.rtu.lv/science/en/publications/17930/fulltext
3. Toy Spirograph. National Museum of American History, Available at: https://americanhistory.si.edu/collections/search?edan_q=spirograph
4. Spirograph. Available at: https://en.wikipedia.org/wiki/Spirograph
5. U. Abel, L. Beukemann and V. Kushnirevych (2017):. Rolling Curves: An Old Proof of the Roulette Lemma. The American Mathematical Monthly, October 2017, Vol. 124, No. 8 pp. 723-736 Available at: https://www.tandfonline.com/doi/abs/10.4169/amer.math.monthly.124.8.723
6. Dan Zwillinger (Edtd.), *Standard Mathematical Tables and Formulas*, 30th Edition, 2003, CRC Press.
7. Deferent and Epicycle, Available at: https://en.wikipedia.org/wiki/Deferent_and_epicycle
8. Gerd Breitenbach. Curves of planetary motion in geocentric perspective: Epitrochoids. Available at: http://gerdbreitenbach.de/planet/planet.html
9. Ya-feng He, Wei-hua Gong, Yong-liang Zhang, Fu-Cheng Liu (2014): Cycloid motions of grains in unmagnetized dust plasma, J.Physics, Vol.12, 2014. Available at: https://arxiv.org/pdf/1407.7962v1.pdf
10. M. A. Reynolds, A M. T. Shouppe (2010): Closed spirograph-like orbits in power law central potential, American J Physics, 2010. Available at: https://arxiv.org/pdf/1008.0559v1.pdf
11. Luminița DUȚA et.al (2010):, Modeling and simulation of cycloid curves with application in robotics, Fiabilitate și Durabilitate, Oct 2010, Vol. 2, no. 6,pp. 23 – 28 Available at: http://www.utgjiu.ro/rev_mec/mecanica/pdf/2010-02/5_Pascale%20Lucia.pdf
12. Juanjuan Wang and Xueliang Ping (2019): The Design Method of Hypocycloid and Epicycloid of Ball-type Speed Reducer. International Research Journal of Advanced Engineering and Science, 2019,Volume 4. Available at: https://irjaes.com/wp-content/uploads/2020/10/IRJAES-V4N2P477Y19.pdf
13. B. Wang, Y. Geng, J. Chu (2019): Generation and application of hypocycloid and asteroid. Journal of Physics. Conference Series, 1345, Vol.2, 2019. **DOI:** 10.1088/1742-6596/1345/3/032085
14. Panagiotis Tsiotras and Luis Ignacio Reyes Castro (2014): The Artistic Geometry of Consensus Protocols, A. LaViers and M. Egerstedt (eds.), Controls and Art. Springer International Publishing, Switzerland, 2014 https://doi.org/10.1007/978-3-319-03904-6_6
15. A. Biran(2019): Geometry for Naval Architect, Technion: Elsevier, Cambridge, 2019.
16. T. Kobayashi, S. Umeda (2010): A design for pseudo-Anosov braids using hypotrochoid curves. Topology and its Applications, Elsevier, 157 ,2010,pp. 280–289. https://doi.org/10.1016/j.topol.2009.04.061
17. A. Ravankar, A. A. Ravankar, Y. Kobayashi, E. Takanori(2016): SHP: Smooth hypocycloidal paths with collision-free and decoupled multi-robot path planning. International Journal of Advanced Robotic Systems, 13, 133 , 2016. https://doi.org/10.5772/63458
18. V. Grill, H. Drexel, W. Sailer, M. Lezius, T.D. Märk(2001): The working principle of the trochoidal electron monochromator revisited. International Journal of Mass Spectrometry, Vol.205, Issues 1–3, 2001. https://doi.org/10.1016/S1387-3806(00)00378-X
19. Yen-Kheng Lim (2020): Hypocycloid motion in the Melvin magnetic universe. PHYSICAL REVIEW D. , **101**, 104031. https://journals.aps.org/prd/abstract/10.1103/PhysRevD.101.104031

20. A. Viviani (1980): Experimental and Theoretical Study of Hypocycloidal Motors with Two-Harmonic Field Windings. in *IEEE Transactions on Power Apparatus and Systems*, vol. PAS-99, no. 1, pp. 292-300, Jan. 1980. DOI: 10.1109/TPAS.1980.319638
21. T. Theobald, T. De Wolff (2014): Norm of Roots of Trinomials, 2014, Available at: https://arxiv.org/abs/1411.6552.
22. K. Etemad, S. Carpendle, F.F. Samavati (2014): Spirograph inspired visualization of ecological networks**.** Proceedings of Conference on Computational Aesthetics 2014, Vancouver, Canada. https://doi.org/10.1145/2630099.2630108
23. Lin Y., Vuillemot R (2013): Spirograph designs for ambient display of tweets. Proceedings of the IEEE VIS Arts Program (VISAP),2013. Available at: http://visap.uic.edu/2013/papers/Lin_Spirographs.pdf
24. Panagiotis Tsiotras (2012): Note on the consensus protocol with some applications to agent orbit pattern generation. Article in Springer Tracts in Advanced Robotics.
25. P. Pathalamuthu, A. Siddharthan, V. R. Giridev(2019): Spirograph based electrospinning system for producing fibre mat with near uniform mechanical property. Indian Journal of Fiber & Textile Research, Vol. 44, September 2019, pp. 279-285 DOI: https://discovery.ucl.ac.uk/id/eprint/10111807/
26. Clark Hochgraf (2016): MAKER: Spirograph-Style Drawing Machine Controlled by Arduino. Proc. Of ASEE's 123rd Conference & exposition, New Orleans, Jan.16.
27. O.Li. SpiroBot: Educational Arduino based polar geometry drawing system, Available at: https://hackaday.io/project/7064-spirobot
28. Robin Roussel (2020): .Crafting Chaos: Computational Design of Contraptions with Complex Behavior. PhD Thesis, 2020, Department of Computer Science University College London.Available at: https://discovery.ucl.ac.uk/id/eprint/10111807/
29. V. Luana (2006):. Plotting the spirograph equations with 'gnuplot', Vol. 133, Linux Gazette, December 2006. Available at https://linuxgazette.net/133/misc/luana/spirograph.pdf
30. Xuan Yao Xinyue Zhang (2015):. Simulating the Spirograph Works by the Geometer's Sketchpad. Proceedings of the 20th Asian Technology Conference in Mathematics, Leshan, China.Available at: https://atcm.mathandtech.org/EP2015/full/7.pdf
31. Attila K¨orei and Szilvia Szilagyi (2022):. Displaying parametric curves with virtual and physical tools. The teaching of mathematics, Vol. XXV, No. 2, pp. 61–73, 2022. Available at: http://elib.mi.sanu.ac.rs/files/journals/tm/49/tmn49p61-73.pdf
32. R. J. Whitaker (1988): Mathematics of the Spirograph. School Science and Mathematics,1988, 88(7): 554-564 https://doi.org/10.1111/j.1949-8594.1988.tb11854.x
33. Deck, Karin M (2099): Spirograph® Math. Humanistic Mathematics Network Journal: Iss, 1999, 19, Article 7. Available at: http://scholarship.claremont.edu/hmnj/vol1/iss19/7
34. Wooi-Nee Tan et al(2015): Transformation matrices in generation of circular patterns. Journal Teknologi (Sciences & Engineering), 2015, 77:18,pp.125–132 **DOI:** https://doi.org/10.11113/jt.v77.6542
35. MacTutor Index. Available at: https://mathshistory.st-andrews.ac.uk/Curves/Rhodonea/
36. Ranjit Konkar(2022): Flattening the Curve. . . of Spirographs. Recreational Mathematics Magazine, June 2022, 9(16):1-20. https://doi.org/10.2478/rmm-2022-0001
37. Robert Connelly and Luis Montejano (2018): Straight Line motion with rigid sets, Beitr Algebra Geom., 2018 doi: 10.1007/s13366-017-0353-7
38. Baccouch M, Dodds S(2020): A Two-Link Robot Manipulator: Simulation and Control Design. International Journal of Robotic Engineering. 5(2),2020. https://doi.org/10.35840/2631-5106/4128
39. Donald H. House, J.C. Keyser (2017): Foundations of Physically Based Modeling and Animation. CRC Press, pp.335-339, 2017.

Authors Profile

Rajkishore Prasad, is a teacher of Electronic Science and have been working as the Principal of B.N. College, Patna under the Patna University, Bihar for last many years. He earned his Ph.D. in the Electronic Science and D.Eng. in Information Science from Japan. He also availed Post-Doctoral Research Fellowship of JSPS at UEC, Japan. His research interest includes area of signal processing, AI and Robotics, Agro-informatics etc. He keeps interest in the investigation of scientific values of tradition and practices being observed in different civilizations. Previously, he was associated with the Post-Graduate Deptt. of Electronic Science, B.R.A. Bihar University, Muzaffarpur, Bihar.

Mr. Shivanshu Raj is currently student of SRM University AP from where he is doing B.Tech in Computer Engineering. He is interested in making higher study and research in the area of AI, Machine Vision, and development of artificially intelligent systems.